

Transmission performance of 90°-bend optical waveguides fabricated in fused silica by femtosecond laser inscription

JING LV,^{1,2} JING BAI,² KAIMING ZHOU,^{2,3} XUESONG MEI,¹ KEDIAN WANG,¹ MING LI,^{1,2} AND GUANGHUA CHENG,^{2,*}

¹State Key Laboratory for Manufacturing Systems Engineering, School of Mechanical Engineering, Shaanxi Key Laboratory of Intelligent Robots, Xi'an Jiaotong University, Xi'an 710049, China

²State Key Laboratory of Transient Optics and Photonics, Xi'an Institute of Optics and Precision Mechanics, Chinese Academy of Sciences, Xi'an 710119, China

³Aston Institute of Photonic Technologies, Aston University, Birmingham, B4 7ET, UK

*Corresponding author: gcheng@opt.ac.cn

Received XX Month XXXX; revised XX Month, XXXX; accepted XX Month XXXX; posted XX Month XXXX (Doc. ID XXXXX); published XX Month XXXX

The L-shape waveguide was written in fused silica using femtosecond laser with beam shaping. The guiding structure supports good light turning, 0.88 dB/turn was achieved at the silica-air interface. By using finite-different time-domain (FDTD) method, the turn loss due to the turning structure and refractive index of the L-shape waveguide has been simulated. The results show that the proposed method has unprecedented flexibility in fabricating 90°-bend waveguide. © 2017 Optical Society of America

OCIS codes: (130.3120) Integrated optics devices; (260.6970) Total internal reflection; (130.2755) Glass waveguides; (140.7090) Ultrafast lasers.

<http://dx.doi.org/>

Nowadays, the direct femtosecond-laser writing technique, which is effectively three-dimensional (3D) micromachining method in transparent materials, has been regarded as a powerful tool in the field of integrated photonic [1,2]. The trend of miniaturization of photonic devices has revolutionized the deployment regimes of most optical devices. As the basic optical components, waveguides with bending structures are expected to shrink the device size and have significant applications. For instance, 90°-bend waveguides have been encouraged to use for deformed ring cavity [3] and optical interconnection [4]. However, there remains challenging on the end product of 90°-bend waveguides, especially femtosecond-laser-written waveguides. Bend waveguides made by femtosecond laser are restricted in size due to the weaker confinement of guided light caused by the low refractive index contrast (on the order of $10^{-2} - 10^{-4}$ [5-7]). Recently, though s-curve waveguides with the radii of more than 10 mm were fabricated and reported [8], no bending efficiency mentioned. For low-index waveguides, waveguide loss increases

exponentially inversely with the bend radius [9]. To overcome these problems, the method of internal total reflection (ITR) on an interface is proposed to allow a drastic reduction in the bending size and ensure low turn loss. However, etching the air trench as a mirror is a complex and expansive process [10]. Thus, we attempt to directly utilize the refractive index contrast between the substrate with special shape and air media to achieve light turning.

In this letter, we report on for the first time to the best of our knowledge the fabrication of femtosecond-laser-written 90°-bend, namely, L-shape waveguides in fused silica based on the ITR principle at silica-air interface. Applying FDTD method to several two-dimensional (2D) bend structures, we demonstrate theoretically the feasibility to write bend waveguides by femtosecond laser inscription technique, thus showing an intriguing potential as compact integrated optical devices such as splitters, optic gyro, and so on.

The waveguides were inscribed into the fused silica glass (Corning 7980-5F) which was a right prism with a height of 5 mm and a base of isosceles right triangle whose leg length was 10 mm. The experiments were performed using a Ti:Sapphire regenerative amplifier femtosecond laser system (Phidia, Uptek Solutions) emitting 50 kHz repetition rate Gaussian laser pulses of pulse width $\tau_p=150$ fs, centred at 780 nm. The pulse energy was attenuated by a half-wave plate in front of a polarizer. **The new combination of a slit [11] and couple of cylindrical lenses [12] was used for beam shaping to produce waveguides with circular cross sections. Because the laser power is severally attenuated if a slit is only used, even though it allows free adjustment to the required beam shape; however, the cross section of the waveguide cannot be optimized when the special cylindrical lenses are used alone without too much energy loss. Therefore, this combination can flexibly adjust the cross section of the waveguide on the premise of low-loss incident laser.** The samples were moved transverse to the incident laser beam by a computer-controlled 3D translation stage (ANT130, Aerotech) which can provide deep sub-micron scale precision over the cubic centimeter scale workspace. The combination of a positive optical phase-contrast microscopy

(PCM) system and a charge coupled device (CCD) connected to a computer was employed to reveal the morphological characteristics of structures in real time. The schematic of experimental setup is shown in Fig. 1.

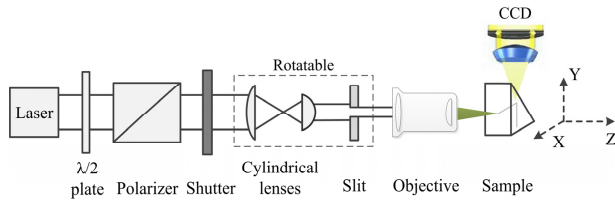


Fig. 1. Schematic of the experimental setup.

The single-scan waveguide writing was investigated for the experimental setup. The waveguide performances depend sensitively on materials characteristics and laser processing parameters [13]. Therefore, the pulse train was focused inside the glass sample to a depth of 150 μm below the polished surface using a 20 \times microscope objective with a numerical aperture of NA=0.42. **Cylindrical lenses pair with the focus of 150mm and 50mm were used.** A slit width of 500 μm was set in the following experimental works. In order to **obtain** the optimum parameters for this material, a range of pulse **energy** from 1.0 to 2.0 μJ and writing velocity from 25 to 500 $\mu\text{m/s}$ were investigated. Assisted by the 3D stage, the intersecting point of the two waveguides (L-shape waveguide) which are perpendicular to each other was placed on the hypotenuse of glass cross-section. This configuration achieved total internal reflection so that the beam can be easily bended 90°. Waveguides were illuminated using a fiber laser of 976 nm. The near field of the guided modes was imaged with a 5 \times microscope objective on the sensor of a CCD camera.

Propagation losses were measured for all the fabricated waveguides by coupling fiber laser to the waveguides with pitch and yaw adjustment carefully. The output power after propagation through the waveguide with different lengths was measured based on the cut-off method. It was found that for single-scan waveguides, in general, the propagation loss decreased first and then increased as both the velocity and pulse energy increased. As a result, the optimal single-scan waveguide with the lowest propagation loss about 0.6 dB/cm at 976 nm was fabricated using a translation velocity of 100 $\mu\text{m/s}$ and a pulse energy of 1.6 μJ . It is important to note that the pulse energy was measured before focusing. The mode field of this waveguide was symmetrical with a horizontal diameter (full width at half maximum) of 7.5 μm and a vertical diameter of 7.7 μm , as shown in Fig. 2. The propagation loss was 2.6 dB/cm at a pulse energy of 2.0 μJ and a velocity of 100 $\mu\text{m/s}$. Results indicate that the waveguide with good performance can be fabricated only within a narrow energy window. For a given pulse energy, as the scanning velocity increased, the refractive index contrast in irradiated region became smaller due to the decrease of accumulated energy per unit area.

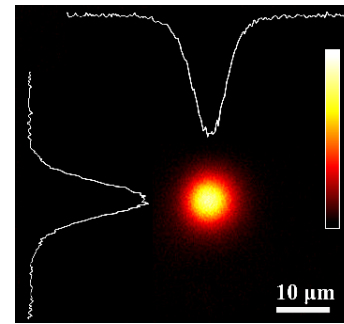


Fig. 2. Near-field mode image of the waveguide written under optimal conditions at 976 nm.

Next, we employed the optimized process parameters to fabricate L-shape waveguides. It is worthy of noting that the writing direction must **be consistent with** the axes of the slit and cylindrical lenses. Therefore the slit and cylindrical lenses had to be rotated by 90° for fabrication of the second waveguide which is perpendicular to the first one. Hypotenuse of glass cross-section, where the two arms of the L-shape waveguide intersect, was polished as aftermath-treatment to improve the interface smoothness. Characterizations of the L-shape waveguide are shown in Fig. 3. The near-field mode was remarkably similar to the straight waveguide's (horizontal diameter of 7.3 μm and a vertical diameter of 7.9 μm), unlike a shift of the mode profile observed in Ref. 8, where higher order modes were excited especially for the waveguides with $R \leq 60$ mm. A larger refractive index change at the inner curve of the outer track resulted in the observed mode shift as well as the deformation [8]. This phenomenon becomes obvious with smaller radius and also be observed in bent fibers [14]. The intersecting position of L-shape waveguides cannot be easily imaged under PCM due to the incident light through two mediums with different refractive indices, shown in Fig. 3(b). The measured bending efficiency is about 81.6% (turn loss is ~ 0.88 dB/turn). The turn loss may be attributed to interface roughness and the intersecting position (the length of Δw) shown in Fig. 3(a). Moreover, the angle between right-angle side and hypotenuse cannot be strict 45°. Because of the limited machining precision, a small amount of light **may** eventually leak out from the inclined surface.

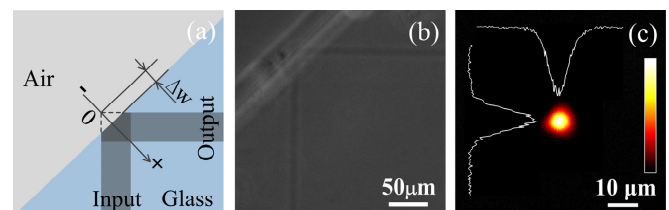


Fig. 3. (a) The definition of the parameter Δw in L-shape waveguide structure; (b) the morphology of L-shape waveguide captured by PCM; (c) near-field distribution of guided laser at 976 nm.

Fig. 3(a) shows the schematic diagram of the experimentally established structure. The refractive index of glass substrate n_s is 1.458 at the wavelength $\lambda=976$ nm. The maximum refractive index change induced by femtosecond laser system is on the order of $10^{-3} - 10^{-4}$. Therefore, it is considered to be a single-mode waveguide. The refractive index contrast is gradual. Because the beam spot intensity is Gaussian distribution. The excitation of the fundamental mode of light intensity for weak-guide optical waveguides can be described by scalar wave equation [15],

$$\nabla^2 \Psi(x, y) + [k^2 n^2(x, y) - \beta^2] \Psi(x, y) = 0 \quad (1)$$

Where $\Psi(x, y)$ is electric field intensity which is proportional to the square root of light intensity $I(x, y)$; β is the propagation constant; k is the wavenumber which equals $2\pi/\lambda$, and $n(x, y)$ represents the refractive index of the waveguide. We deduce the equation to calculate the refractive index change $\Delta n(x, y)$ of laser-irradiated areas,

$$\Delta n(x, y) \approx -\frac{\lambda^2}{16\pi^2 n_s I} \left[\nabla^2 I - \frac{1}{2I} (\nabla I)^2 \right] \quad (2)$$

It should be noted that the effective index used in the formula derivation is approximately equal to n_s . The Gaussian fitting of the calculated value of the refractive index contrast $\Delta n(x, y)$ of single axis was used in numeric calculation.

A 2D waveguide model with perfectly matched layer condition is applied. The source with TE fundamental mode is injected into the input waveguide. Due to dramatic change of the electromagnetic field in the turn region, it needs to improve the accuracy of simulation using the thinning grids method. Maybe some higher-order modes would exist in the output field of L-shape waveguides, but can be theoretically consumed up if the length of the waveguide is infinite. Therefore, the bend efficiency is lower than a power ratio of the output to the input. We compute the fraction of the power from mode-in that can propagate in mode-out based on the overlap method between the output field and input field.

In this section, we evaluate the impact of Δw in the waveguide structure, which is determined by the intersecting position as unclearly shown in Fig. 3(b), to the bend performance and the results are in Fig. 4(a). The field distribution from the output waveguide has almost no changes compared to that of the input waveguide as displayed in Fig. 4(b). The L-shape waveguide has great optical performance without obvious mode shift even though its size is on the order of microns. The maximum bending efficiency is $\sim 97.3\%$ at $\Delta w = 8.29 \mu\text{m}$, which can compensate the Goos-Hanchen shift at the interface. It is worth noting that bending efficiency is larger than 80.0% when Δw is in the range from 6.11 to 10.40 μm , i.e. $\sim \pm 2 \mu\text{m}$ from the optimized position. Bending efficiency becomes $\sim 50.0\%$ when Δw is 4.18 μm or 12.39 μm . The lower bending efficiency of 81.6% in the experiment than the maximum value of numerical simulation, can be attributed to the undesired intersecting position and angle of inclined plane. The scattering of optical waves at the isosceles of the prism (glass-air boundary) is another dominant source for loss due to high electromagnetic field values at the interface (red region in Fig. 4(b)). However, we can deduce that the processing error is less than 2 μm . More remarkable, the structural tolerance becomes increasingly strict with the increase of the value of refractive index contrast, shown in Fig. 4(a). L-shape waveguide with larger index contrast requires more accurate position of the reflection surface. Because the bigger the numerical aperture, the smaller the mode field and larger divergence angle. Its tolerance limits get looser to reduce the processing difficulty when index contrast Δn_2 is half value of Δn_1 (bending efficiency is greater than 80.0% within the optimum position plus or minus $\sim 3 \mu\text{m}$). It is feasible for femtosecond laser precision machining to satisfy the demand of micro-meter accuracy [16], so that the intersecting position can be controlled in a very small range. Our approach creates a completely new platform for the fabrication of 3D bend waveguide, offering an important reference for integrated optical circuits.

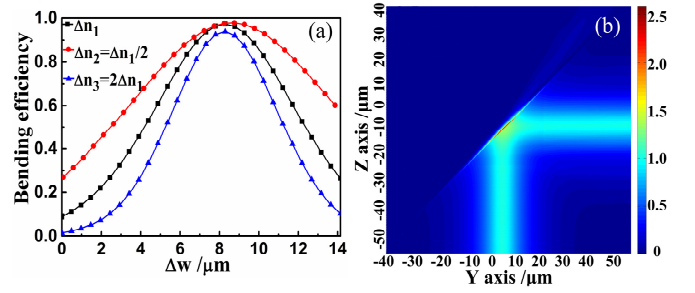


Fig. 4. (a) Bending efficiency of L-shape waveguide for different Δw at $\lambda=976 \text{ nm}$. The index contrast Δn_1 calculated on the basis of the near-field mode distribution in Fig. 2; (b) Electric-field intensity at the global maximum point of $\Delta w=8.29 \mu\text{m}$ with index contrast Δn_1 .

The two waveguides are not completely intersected taken into consideration the Goos-Hanchen shift in our case. The lengths of their extensions (ΔH in Fig. 5(a)) range from 0 to 150 μm herein. Fig. 5(b) shows the dependence of the bending efficiency on ΔH . Initially, small ΔH (ΔH for waveguides with index contrast of Δn_1 , Δn_2 and Δn_3 are ~ 30 , 50 and 20 μm , respectively) has little impact on the bending efficiency. As the extended line increases, the bending efficiency decreases monotonically. Declining is accelerated when index contrast increases. During the length of 150 μm , the bending efficiencies are $\sim 93\%$ and 66% for smaller and larger index contrasts, respectively. These phenomena can be explained as follows. The emergence of the incident light from the optical waveguide has Gaussian divergence, which beam waist is at its port. Using $\text{NA} = (n_1^2 - n_2^2)^{1/2}$, the numerical aperture can be estimated with knowledge of the refractive index of the waveguide region (n_1) and the unmodified glass (n_2). The bigger refractive index of the waveguide core causes higher NA and smaller mode field diameter. Rayleigh length is proportional to the square of the beam waist radius. Therefore, the flattening part of the efficiency curve in the early stage roots in the distribution of modal field out from the waveguide. The light from the waveguide with smaller index contrast has less divergence angle and less loss. It is obvious that the influence of ΔH on bending efficiency is less than the parameter of Δw , because of dramatic change of the electromagnetic field and its strong intensity distribution in the turn region. Femtosecond laser inscription is suitable for achieving higher bending efficiency for the L-shape waveguide structure. Because the index contrast induced by femtosecond laser is small and controlled with process parameters.

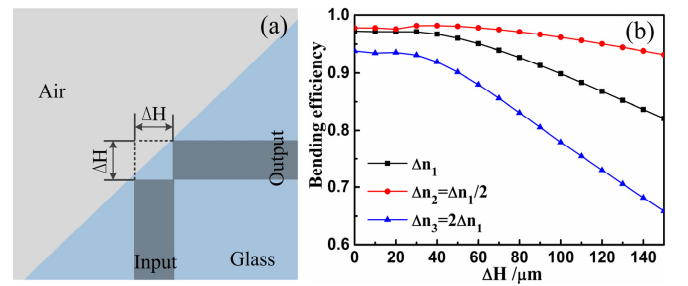


Fig. 5. (a) Diagram of the definition of ΔH in L-shape waveguide structure; (b) bending efficiency versus the length of extended line ΔH at $\lambda=976 \text{ nm}$; the index contrast Δn_1 calculated on the basis of the near-field mode distribution in Fig. 2.

In summary, the straight single-scan waveguides and L-shape waveguides were fabricated in fused silica by the shaped femtosecond laser beam. The good mode-field distribution and low transmission loss were obtained. The guiding structures support good light confinement with a translation velocity of 100 $\mu\text{m/s}$ and a pulse energy of 1.6 μJ , yielding propagation loss of ~ 0.6 dB/cm at 976 nm. Bending efficiency of L-shape waveguide was measured to be $\sim 81.6\%$. Using 2D waveguide models, the bending efficiency is strongly dependent on device geometry, especially the intersecting position. That is, ± 2 μm deviating from the optimized position can lead to **$\sim 20\%$ reduction in bending efficiency**. The acceptable range of the extensions is within 30 μm . It is feasible for femtosecond laser precision machining to satisfy the demand of micro-meter accuracy. Our novel approach will facilitate the integration of high-density optical circuits. Future effort **will be** writing mirror inside materials so that beam turning is no longer dependent on the shape of samples and can be at a more arbitrary position.

Funding. National Natural Science Foundation of China (NSFC) (61378019, 51375374), the Program for Chang Jiang Scholars and the Innovative Research Team in University (IRT_15R54), National Key Research And Development Program (2016YFB1102501).

References

1. R. R. Gattass and E. Mazur, *Nat. Photonics* **2**, 219 (2008).
2. R. Osellame, H. J. W. M. Hoekstra, G. Cerullo, and M. Pollnau, *Laser Photonics Rev.* **5**, 442 (2011).
3. T. Ling, L. Liu, Q. Song, L. Xu, and W. Wang, *Opt. Lett.* **28**, 1784 (2003).
4. N. Bamiedakis, R. Penty, and I. H. White, *J. Lightwave Technol.* **31**, 2370 (2013).
5. S. M. Eaton, M. L. Ng, R. Osellame, and P. R. Herman, *J. Non-cryst. Solids* **357**, 2387 (2011).
6. L. Shah, A. Y. Arai, S. M. Eaton, and P. R. Herman, *Opt. Express* **13**, 1999 (2005).
7. A. Ródenas, G. A. Torchia, G. Lifante, E. Cantelar, J. Lamela, F. Jaque, L. Roso, and D. Jaque, *Appl. Phys. B* **95**, 85 (2009).
8. T. Calmano, A. Paschke, S. Müller, C. Kränkel, and G. Huber, *Opt. Express* **21**, 25501 (2013).
9. H. Nishihara, M. Haruna, and T. Suhara, *Optical Integrated Circuits* (New York, 1989).
10. Y. Qian, S. Kim, J. Song, G. P. Nordin, and J. Jiang, *Opt. Express* **14**, 6020 (2006).
11. M. Ams, G. D. Marshall, D. J. Spence, and M. J. Withford, *Opt. Express* **13**, 5676 (2005).
12. G. Cerullo, R. Osellame, S. Taccheo, M. Marangoni, D. Polli, R. Ramponi, P. Laporta, and S. De Silvestri, *Opt. Lett.* **27**, 1938 (2002).
13. M. Thiel, G. Flachenecker, and W. Schade, *Opt. Lett.* **40**, 1266 (2015).
14. R. W. Smink, B. P. de Hon, and A. G. Tjhuis, *J. Opt. Soc. Am. B* **24**, 2610 (2007).
15. W. C. Chew, *Waves and fields in inhomogeneous media* (New York, 1995), Vol. 522.
16. M. Malinauskas, A. Žukauskas, S. Hasegawa, Y. Hayasaki, V. Mizeikis, R. Buividas, and S. Juodkakis, *Light Sci. Appl.* **5**, e16133 (2016).

References for review

1. R. R. Gattass and E. Mazur, "Femtosecond laser micromachining in transparent materials," *Nat. Photonics* **2**(4), 219-225 (2008).
2. R. Osellame, H. J. W. M. Hoekstra, G. Cerullo, and M. Pollnau, "Femtosecond laser microstructuring: an enabling tool for optofluidic lab-on-chips," *Laser Photonics Rev.* **5**(3), 442-463 (2011).
3. T. Ling, L. Liu, Q. Song, L. Xu, and W. Wang, "Intense directional lasing from a deformed square-shaped organic-inorganic hybrid glass microring cavity," *Opt. Lett.* **28**(19), 1784-1786 (2003).
4. N. Bamiedakis, R. Penty, and I. H. White, "Compact multimode polymer waveguide bends for board-level optical interconnects," *J. Lightwave Technol.* **31**(14), 2370-2375 (2013).
5. S. M. Eaton, M. L. Ng, R. Osellame, and P. R. Herman, "High refractive index contrast in fused silica waveguides by tightly focused, high-repetition rate femtosecond laser," *J. Non-cryst. Solids* **357**(11), 2387-2391 (2011).
6. L. Shah, A. Y. Arai, S. M. Eaton, and P. R. Herman, "Waveguide writing in fused silica with a femtosecond fiber laser at 522 nm and 1 MHz repetition rate," *Opt. Express* **13**(6), 1999-2006 (2005).
7. A. Ródenas, G. A. Torchia, G. Lifante, E. Cantelar, J. Lamela, F. Jaque, L. Roso, and D. Jaque, "Refractive index change mechanisms in femtosecond laser written ceramic Nd:YAG waveguides: micro-spectroscopy experiments and beam propagation calculations," *Appl. Phys. B* **95**(1), 85-96 (2009).
8. T. Calmano, A. Paschke, S. Müller, C. Kränkel, and G. Huber, "Curved Yb:YAG waveguide lasers, fabricated by femtosecond laser inscription," *Opt. Express* **21**(21), 25501-25508 (2013).
9. H. Nishihara, M. Haruna, and T. Suhara, *Optical Integrated Circuits* (New York, 1989).
10. Y. Qian, S. Kim, J. Song, G. P. Nordin, and J. Jiang, "Compact and low loss silicon-on-insulator rib waveguide 90° bend," *Opt. Express* **14**(13), 6020-6028 (2006).
11. M. Ams, G. D. Marshall, D. J. Spence, and M. J. Withford, "Slit beam shaping method for femtosecond laser direct-write fabrication of symmetric waveguides in bulk glasses," *Opt. Express* **13**(15), 5676-5681 (2005).
12. G. Cerullo, R. Osellame, S. Taccheo, M. Marangoni, D. Polli, R. Ramponi, P. Laporta, and S. De Silvestri, "Femtosecond micromachining of symmetric waveguides at 1.5 μm by astigmatic beam focusing," *Opt. Lett.* **27**(21), 1938-1940 (2002).
13. M. Thiel, G. Flachenecker, and W. Schade, "Femtosecond laser writing of Bragg grating waveguide bundles in bulk glass," *Opt. Lett.* **40**(7), 1266-1269 (2015).
14. R. W. Smink, B. P. de Hon, and A. G. Tjhuis, "Bending loss in optical fibers—a full-wave approach," *J. Soc. Am. B* **24**(24), 2610-2618 (2007).
15. W. C. Chew, *Waves and fields in inhomogeneous media* (IEEE Press, New York, 1995), Vol. 522.
16. M. Malinauskas, A. Žukauskas, S. Hasegawa, Y. Hayasaki, V. Mizeikis, R. Buividas, and S. Juodkazis, "Ultrafast laser processing of materials: from science to industry," *Light Sci. Appl.* **5**(8), e16133 (2016).